The glymphatic system and its role in cerebral homeostasis

Invited Mini-Review for Journal of Applied Physiology

Title: The Glymphatic System and Its Role in Cerebral Homeostasis

Key words: Glymphatic system, cerebrospinal fluid, interstitial space, MRI, state of arousal

Authors: Helene Benveniste[1], Rena Elkin[2], Paul Heerdt[1], Sunil Koundal[1], Yuechuan Xue[1], Hedok Lee[1], Joanna Wardlaw[4] and Allen Tannenbaum[2]

Affiliations: [1]Department of Anesthesiology
Yale School of Medicine
330 Cedar Street
New Haven, CT

[2] Departments of Computer Science and Applied Mathematics
Stony Brook University
Stony Brook New York

[3] Brain Research Imaging Centre,
Centre for Clinical Brain Sciences,
Dementia Research Institute at the University of Edinburgh, Edinburgh, United Kingdom

Correspondence: Helene Benveniste, MD, PhD
Department of Anesthesiology
helene.benveniste@yale.edu

Acknowledgements: NIH R01AG048769, RF1 AG053991, R01AG057705 and Leducq Foundation (16/CVD/05)

Abstract

The brain's high bioenergetic state is paralleled by high metabolic waste production. Authentic lymphatic vasculature is lacking in brain parenchyma. Cerebrospinal fluid (CSF) flow has long been thought to facilitate central nervous system detoxification in place of lymphatics, but the exact processes involved in toxic waste clearance from the brain remain incompletely understood. Over the past 8-years, novel data in animals and humans have begun to shed new light on these processes in the form of the "glymphatic system", a brain-wide perivascular transit passageway dedicated to CSF transport and interstitial fluid exchange that facilitates metabolic waste drainage from the brain. Here we will discuss glymphatic system anatomy, methods to visualize and quantify GS transport in the brain and also discuss physiological drivers of its function in normal brain and in neurodegeneration.

Introduction

The brain's high energy demand is paralleled by high metabolic waste production. In most body organs the lymphatic vasculature is responsible for metabolic waste drainage and fluid homeostasis. While the meninges covering the brain and spinal cord are equipped with lymphatics (3, 4, 69), the brain parenchyma itself is devoid of lymphatic vessels. The tight blood brain barrier (BBB) restricts solute and large fluid shifts and alternate waste elimination systems are operational in brain tissue. Cerebrospinal fluid (CSF) produced in the choroid plexuses of the cerebral ventricles, in addition to other roles, is thought to play an important role for detoxification of brain tissue in place of lymphatics (19, 20, 58, 89). The "glymphatic system" concept was brought to prominence 2012 (47) shedding new light on CSF transport and brain waste drainage processes. The glymphatic system (GS) is described as a perivascular transit passageway for CSF and interstitial fluid (ISF) exchange that facilitates metabolic waste drainage from the brain parenchyma in a manner dependent on aquaporin 4 (AQP4) water channels on glial cell (47). Several excellent reviews of the GS are available, and we refer readers to these for more details (1, 9, 46, 77, 99, 103). Here we will focus on 1) GS anatomy, 2) methods to visualize and quantify GS transport in the brain and 3) discuss physiological drivers of GS function in normal brain and in the setting of neurodegeneration.

Composition of the glymphatic system

The GS is located beyond the BBB and comprises the entire peri-vascular space (PVS) within the brain parenchyma (47). The PVS is constructed as a coaxial system where the inner cylinder is the BBB-tight vessel (e.g. artery, arteriole, capillary, venule, or vein) and the outer cylinder is made of astrocytic end-feet processes which envelop the entire cerebral vasculature. The outer perimeter of the PVS is not 'tight' due to gaps (20-30 nm) between the astrocytic end-feet

processes (74). The cortical penetrating arterioles are surrounded in part by a layer of pia mater, and at this level the PVS is a fluid filled space referred to as the Virchow-Robbin space, from where it eventually merges into the basal lamina at the level of the capillary. The basal lamina is located in between the vessel wall and the astrocytic end-feet. Under normal conditions, the capillary cell types do not make direct contact with the PVS and are always separated by the basal lamina (82, 89). In humans, the PVS can be detected in the brain parenchyma by magnetic resonance imaging (MRI) as tube-like structures which run perpendicular to the brain's surface in directions that are spatially correlated with perforating vessels thought to be primarily arterial (51, 106). Cortical PVS can be observed in young, healthy brain (**Fig. 1**) but are more common in the aging brain and abnormally dilated PVS are associated with cerebral small vessel disease (cSVD) and other neurological disease states (26, 106, 107). In the human and rodent brain, the PVS communicates with the subarachnoid space as evidenced by multiple studies showing that tracer uptake is visible in PVS following *in vivo* administration of tracers into CSF (vide infra).

Rapid transport of tracers from CSF into the parenchymal perivascular network under carefully controlled physiological conditions was documented in early work by Rennels and coworkers in cat brain by administering horse radish peroxidase into CSF (89). Two decades later, CSF and solute transport along the PVS of pial arteries and cortical penetrating arterioles of live mice was visualized in real time using 2-photon microscopy by administering fluorescently tagged dyes into the cisterna magna (47). These pioneering *in vivo* studies revealed that small molecular weight (MW) solutes moved rapidly (5-10 min) into the peri-arterial space (but not peri-venous space) and from there into the ISF space (47). Furthermore, waste solutes including soluble $A\beta_{1-40}$ injected into brain parenchyma was shown to migrate from the ISF into the PVS of the large central veins inferring that peri-venous conduits served as exit pathways connecting to lymphatic

networks outside the brain. Importantly, it was also documented that the astrocytic AQP4 water channels were important for rapid peri-arterial influx of CSF and solutes as well as for drainage of soluble Aβ (47). The importance of the AQP4 water channels for rapid CSF-ISF exchange has been contested (1, 76, 100), and alternate physiological factors (e.g. ISF volume changes and vascular pulsatility) may be more important for time efficient GS transport and waste drainage (vide infra). It is also not known exactly how the AQP4 water channels regulate GS function. Recently, a novel study using multiple echo time arterial-spin-labeling MRI demonstrated slower than normal water exchange times in the brain (suggesting slow water transport across the PVS into parenchyma) in transgenic mice models lacking AQP4 water channels compared to mice with normal AQP4 water channels (80). **Fig. 2** is an illustration of the principal anatomical components of the GS and highlights that in normal brain solutes in the ISF drain towards the peri-venous space.

Whole brain GS function

To visualize and quantify GS function in the whole rodent brain we administered paramagnetic gadolinium-tagged contrast molecules into CSF of the rat via the cisterna magna in combination with dynamic contrast enhanced magnetic resonance imaging (DCE-MRI) (45). The paramagnetic contrast agents shorten the T1 relaxation time thereby eliciting signal changes on the T1-weighted MRIs enabling tracking of solute transport in CSF and brain parenchyma (45). Using this approach, we demonstrated that small MW paramagnetic contrast molecules moved rapidly in the subarachnoid space, along pial arteries and more slowly transited into brain parenchyma in a specific anatomical pattern (45). We noted that brain regions with the most rapid CSF and solute transport included the brainstem, hypothalamus, olfactory bulb, frontal cortex, cerebellum and the ventral hippocampus (45). We have since refined the MRI based GS

transport technique and determined than only a relatively small (19-20%) fraction of the contrast agent administered into the CSF enters into the rat brain parenchyma over 2.5 hr (66). In addition, we showed that MR contrast influx and clearance from brain parenchyma is dependent on body position (67) and the anesthetic used (8).

The GS transport pattern in the rat brain using DCE MRI is very similar to that observed using the same method in non-human primate brain (37) and humans (28, 29, 92). In humans, intrathecal lumbar administration of MR contrast (Gadobutrol, MW 605 Da) has been performed to diagnose dural tears in otherwise normal subjects (91). In these clinical DCE MRI studies MR contrast enhancement in brain parenchyma was observed in a pattern similar to the rodent brain with largest uptake in areas adjacent to large arteries including the anterior, middle and posterior cerebral arteries (91). In the human brain, regions with most significant uptake after administration of contrast into the lumbar intrathecal space (6-9 hrs) included the brainstem, cerebellum, frontal cortex and limbic regions (hippocampus, amygdala, accumbens, and entorhinal cortex) (91).

Quantification of GS function

As described above, GS transport can be observed in the entire brain using the DCE-MRI approach (8, 45, 66, 67). However, supplementary analysis is required to quantify transport and to extract differences in GS transport flow across brain regions and across experimental groups. Current techniques for quantifying GS transport include assessment of time-signal-curves of brain parenchymal solute uptake or clearance (8, 28, 45), kinetic analysis (67) or k-means cluster analysis (45, 50). These analytical strategies have provided valuable information but are limited because solute transport across brain regions is heterogeneous causing generalized kinetic models to fail.

Visualization of CSF transport into brain using optimal mass transport

We were the first to model GS transport based on DCE MRI images using the traditional optimal mass transport (OMT) formulation (86, 87). The theory of OMT seeks the most feasible way to redistribute mass from one given distribution to another while minimizing the associated cost of transportation (85). In the first approach, we made several assumptions including the notion that glymphatic CSF-solute transport was governed principally by advection (86) as originally proposed (47). These initial results revealed aberrant CSF "streaming" patterns of contrast solutes into brain parenchyma (86). Transport by pure advection has been a subject of controversy surrounding GS transport and several studies have suggested diffusion dominant solute transport in neuropil (82, 100). We further improved the OMT based computational analysis with the ultimate goal of visualizing how PVS pathology might alter GS transport and waste drainage. We introduced a novel visualization framework, "GlymphVIS" (30) using a more physiologically relevant model inspired by the work of Benamou and Brenier (7). Specifically, in the GlymphVIS model we added a diffusion term in the standard continuity equation to better model both advection and diffusion thereby more accurately modelling the CSF-solute transport in the brain parenchyma (for more detail see Elkin et al., (30)). **Fig. 3** shows the effect of increasing the diffusion term in the optimal transport algorithm. With minimal or no diffusion term the OMT presentation of CSF parenchymal streamlines are not aligning with physiological evidence of MR contrast uptake in live rodent brain (**Fig. 3A, arrows**); however with more diffusion weighting (**Fig. 3B**) the aberrant parenchymal CSF pathways have disappeared and the uptake pattern better match what is observed on the MRI data strongly suggesting that parenchymal GS transport is governed by both advection and

diffusion. We have further validated these data using phantoms (61). **Fig. 4A** shows the conventional visualization of glymphatic transport in whole rat brain based on DCE MRIs and '% signal increase from baseline' 1.5 hrs. after administration of MR contrast into the CSF via cisterna magna. The color-coded map shows the spatial distribution of CSF tagged with MR contrast demonstrating that CSF and the contrast solute have penetrated into the cerebellum, midbrain, olfactory bulb and along the PVS of the middle cerebral artery as highlighted in **Fig. 4C**. **Fig. 4B** shows the same data set processed by the GlymphVis algorithm with advection and diffusion terms deriving CSF streamlines created by proximity and similar curvature using the QuickBundles algorithm (35). These streamlines show brain parenchymal CSF flow patterns at a fixed point in time. Please note that the CSF streamlines along the MCA **(Fig. 4D)** are matching contrast uptake in the original data (**Fig. 4C**). We are currently extending the GlymphVIS analysis to include visualization of CSF pathlines. These pathlines represent the time-varying CSF trajectories and can be used to determine particle attributes including solute speed and flux in one comprehensive figure. Moreover, we are exploring and comparing the advantages (and disadvantages) of both Eulerian and Lagrangian coordinates in visualizing the flow (61).

The GS operates more efficiently in the sleeping brain when compared to wakefulness

All the initial experiments on the GS were carried out on mice anesthetized with ketamine/xylazine (47). Nedergaard's team proceeded to test the GS system's functionality in different arousal states and discovered that the GS function differed between sleep and wakefulness (109). Specifically, they discovered that GS influx of solutes into brain parenchyma was increased ~80% by in sleep states compared to wakefulness inferring that the GS system is largely non-functioning in wakefulness (109). Further, drainage of Aβ from brain parenchyma was ~40% more efficient during sleep or anesthesia with ketamine/xylazine (KX) when

compared to wakefulness (109). A dramatic increase in the ISF volume fraction (>40-60%) between sleep and wakefulness controlled by norepinephrine (NE) was discovered and attributed to the enhanced GS function. Specifically, it was suggested that solute transport in the ISF was less restrictive in sleep when compared to wakefulness (109). Collectively these experiments also implied that GS function and waste clearance was inefficient in wakefulness regardless of the presence of AQP4 water channels. Of note, the observed increase in GS transport with KX anesthesia compared to wakefulness was attributed to an associated increase in slow wave delta power and decreased central norepinephrine (NE) tone (109). From these data, one can infer that the enhanced GS transport observed with KX anesthesia was mediated by xylazine and not by ketamine, which is known to increase central NE (57, 63). Xylazine is an alpha-2 receptor agonist and blocks central NE release (75) similar to the hypnotic dexmedetomidine (13, 54) used clinically for sedation and as an adjuvant for general anesthesia. In support of this statement, it was also demonstrated that anesthesia with dexmedetomidine and low dose isoflurane increased GS transport 2-fold when compared to isoflurane alone (8).

GS function and physiological drivers

Rennels and coworkers showed that unilateral carotid artery ligation impeded perivascular influx of CSF and tracer molecules leading them to conclude that normal arterial pulsatility was a major driver (89). Iliff and colleagues validated these data and further showed that an increase in pulsatility with dobutamine enhanced GS transport (48). More recent studies conducted using large 1.0 μm microspheres and direct visualization of the large PVS around pial surface arteries showed that CSF transport was indeed pulsatile and bulk flow driven at the surface of the brain (78). In addition, high pulsatility as observed in acute hypertension was shown to be ineffective in driving solute transport in the PVS (78). Paradoxically, while it appears that the rate of CSF–

ISF exchange and Aβ clearance is highest during non-REM sleep (109), this physiological state is actually associated with periods of significantly reduced blood pressure, cerebral blood flow, and cerebral pulsatility (59, 60, 72, 96). However, the question of whether or not lower magnitude pulsatility might be overall more efficient for GS transport during sleep needs further investigation.

The importance of the spontaneous oscillations in arterial tone and diameter that occur in multiple vascular beds including in the brain for GS function is unknown. Termed "vasomotion" these rhythmic but very low frequency (ranging from ~ 3-25/minute depending upon vessel size) variations in arterial/arteriolar smooth muscle tone can produce fluctuations in vessel diameter comparable to those resulting from cardiac contraction and are influenced by a range of factors including general anesthesia and sedation (18, 43, 49, 64). While not generally considered to play a major role in bulk CSF flow, given the proposed role of the GS and clearance of Aβ, there has been particular interest in the potential relationship between impaired vasomotion and cerebral amyloid angiopathy (25). Notably, a recent study documented that spontaneous vasomotion correlated with perivascular clearance of solutes in live, awake mice and this driving force was impaired in mice with cerebral amyloid angiopathy (104). As with cardiac pulsatility, vasomotion is decreased during non-REM sleep (110). Implications of these findings in terms of GS function remain unclear, but when considered in conjunction with decreased cardiogenic arterial pulsatility during sleep, the data suggest that two physical factors thought to be the main drivers of GS function may actually be diminished when CSF-ISF exchange is highest.

Lymphatic vessels in the meninges

Lymphatic vessels were documented in the cerebral dura mater covering the human brain several decades ago (12). Using newer, state-of-the art imaging techniques and molecular markers of the

lymphatic endothelial cells the meningeal lymphatics were rediscovered in 2015 and thoroughly described in mice both structurally and functionally (4, 69). Meningeal lymphatics were observed using Prox1-GFP and $Vegfr^{3+/LacZ}$ reporter mice and immune-fluorescence in the dura mater surrounding the brain in a particular pattern (4, 69). Specifically, the majority of lymphatic vessels were observed to run toward the base of the skull along the transverse sinus, the sigmoid sinus, the retroglenoid and rostral rhinal vein (4, 21, 69, 71). In areas of the skull foramina, lymphatic vessels could be observed to exit along meningeal portions of internal carotid artery and along cranial nerves (3). In other rodent studies, it was shown that meningeal lymphatics develop and mature after birth and their growth and development is dependent on vascular endothelial growth factor C (VEGF-C) (3). The functionality of the meningeal lymphatics was demonstrated by injecting inert tracers into the brain parenchyma of the Prox1-GFP mice and drainage of the tracer could be located on the meningeal lymphatics and at the level of the deep cervical lymph nodes (4, 69). Further a transgenic mouse with loss of dural lymphatics had reduced macromolecule drainage from the brain, but paradoxically, no increase in intracranial pressure suggesting alternative pathways for fluid and solute drainage (4). A recent post-mortem study in humans confirmed the presence of lymphatic vessels in the dura, however, Aβ deposition in the wall of dural lymphatic vessels was absent (36) suggesting that these drainage pathways (at least in humans) might not be implicated in severe AD pathology.

Intriguingly, lymphatic vessels along the dural sinuses and along meningeal artery can be visualized in human brain after intravenous administration of a MR contrast agent (2). The visualization of lymphatic vessels is based on the fact that after i.v. administration of Gadobutrol, the MR contrast molecule leaks out of the dural blood vessels and travels through the ISF space into adjacent lymphatics (2). By implementation other special MR pulse sequences, the MR

contrast signal from blood can be eliminated and after subtraction the meningeal lymphatics can be revealed. Using this novel *in vivo* approach to study meningeal lymphatics in humans will allow further investigations into the functionality and role of meningeal lymphatics in normal brain and in neurodegenerative disease states.

Glymphatic transport in aging, neurotrauma and neurodegeneration

Brain parenchymal influx of CSF and Aβ drainage from ISF is significantly reduced in old mice when compared to young and middle-aged mice (62). The decline in GS transport function in aging mice is multi-factorial and ascribed to loss of perivascular AQP4 polarization and neuroinflammation (62). GS function has also been shown to be decreased in a mouse model of AD (81), in traumatic brain injury (TBI) (44, 83, 88), and in stroke (34). Glymphatic clearance of tau in the 'hit & run' TBI mouse model, was shown to be reduced acutely after the insult and associated with later onset altered global AQP4 expression and loss of perivascular AQP4 polarization secondary to inflammation (44, 88). Specifically, in the TBI mouse model the temporal trajectories of intracranial pressure changes and tissue edema (peaking 3 days after TBI) were different from those of AQP4 expression changes (peaked at 7-days) post-TBI suggesting that the water channels were not directly related to edema information acutely after TBI (88). To summarize, in conditions of aging, TBI and stroke, the peri-vascular CSF passage through brain tissue is deficient and GS transport and waste drainage is therefore less efficient. However, the underlying pathophysiology of impaired CSF influx in these various pathologies are different. For example, in stroke and TBI, CSF influx is nearly absent in the ischemic/lesioned hemisphere when compared to the contralateral side, secondary to tissue trauma (34), causing loss of vascular pulsatility and tissue edema with obliteration of the peri-

arterial conduits in the parenchyma. In aging, the peri-arterial CSF influx and CSF-ISF exchange is compromised primarily secondary to perivascular inflammation and loss of AQP4 peri-vascular polarization (62).

Glymphatic transport has also been studied in animal models of cerebral small vessel disease (cSVD) (5). cSVD is frequently observed in the elderly human brain and a common cSVD subtype is associated with thickening of the cerebral arterioles – so-called 'arteriolosclerosis'. Arteriolosclerosis can progress to fibrinoid necrosis, microhemorrhage or microinfarction and capillaries are also affected and sometimes venules (32, 55, 97, 107). The pathogenesis of sporadic arteriolosclerosis cSVD is largely unknown but thought to result from hypertension, vasospasm or 'failure of the endothelial barrier function' and ultimately impaired oxygen delivery to the tissues (70, 107). MRI based diagnosis of c SVD include the presence of small subcortical infarcts, white matter hyperintensities (WMH), enlarged PVS, lacunes, microbleeds and cerebral atrophy (22, 107). Thickening of the arterial wall and dilated PVS are thought to impair oxygen delivery to the tissue similar to what is documented in multiple sclerosis where tissue hypoxia is widespread (24, 73) although the precise mechanism is unknown. Rodent models of spontaneous hypertension have been used to investigate the effect of chronic hypertension on cSVD pathology in the brain. While some reports document increased GS bulk-flow driven transport in the spontaneously hypertensive rat (SHR) due to changes in vessel stiffness and arterial pulse wave velocity (6), others report that overall CSF-ISF exchange is reduced (78, 79).

Hypoxia and CSF transport: implications for high altitude sickness

To the best of our knowledge, no animal experiments have investigated the effect of high-altitude hypoxia on GS transport. The potential mechanisms involved in potential GS changes in

high-altitude sickness is discussed below and are based on current evidence of CSF transport in conditions where hypoxia is thought to be implicated (e.g. cSVD, stroke and traumatic brain injury) and inspired by excellent recent reviews by Lawley et al., (65) and Hackett and Roach (40). Further, given the common involvement of deep white matter in high-altitude cerebral edema (HACE) and cSVD we will highlight how peri-vascular transport of CSF might be affected in conditions of acute mountain sickness (AMS) and HACE. Symptoms of AMS include headache, fatigue, nausea and vomiting and sleep disturbance; and the headache component is thought to involve pain transmission via the trigemino-cervical complex like in migraine headache (14). The much more severe condition of HACE is rare but can occur with rapid ascents to altitudes of >4,000m and afflicted subjects have ataxic gait, and altered mentation (40). The prime 'insult' instigating altitude sickness is obviously related to hypoxia; however, it is currently not possible to predict who will be susceptible to developing AMS or HACE (40, 94). A hypothesis proposed states that individual susceptible to high-altitude sickness are those with less intracranial and intraspinal 'compliance' or a lower CSF-to-brain parenchymal tissue volume ratio (94). This hypothesis has been indirectly supported by studies demonstrating that older subjects have a lower incidence of AMS compared to younger subjects at moderate altitude (93) and evidence of higher CSF-to-brain tissue volume in elderly when compared to young adults (39). An in-depth discussion of the CNS 'compliance' hypothesis was recently presented by Lawley et al. (65) and readers are referred to this excellent review for details of the proposed CSF pathophysiology in high-altitude illness. Here, we briefly discuss pathophysiology of AMS and HACE from the point of view of GS transport and brain waste drainage. Assuming that the primary outcome in high altitude illness is rapid onset hypoxia, cerebral overperfusion, increased sympathetic activity and 'brain swelling' secondary to vasodilation, and BBB compromise (in

the setting of HACE) (40) several key points regarding how GS transport might be affected can be inferred:

- **Hypoxic vasodilation and increased cerebral blood flow (CBF)**: Adaptive mechanisms to optimize oxygen delivery during high-altitude hypoxia involve an extraordinary network of direct and reflex pathways that ultimately affect ventilation and hemodynamics. Several clinical studies using MRI and arterial spin labeling pulse sequences have documented significant (~5-20%) increases in CBF (68, 105) in younger subjects with acute exposure to high altitude as well as reduced cerebral vascular reactivity (CVR) (105). Hypoxic arterial vasodilation by MR angiography was confirmed in the human brain at high altitude (68). Further, enlargement of the cerebral venous sinuses by MR venography was also documented in human subjects exposed to a hypoxic challenge (108). Although no study as of yet have investigated solute CSF and parenchymal transport under conditions of high-altitude hypoxia, we have documented impaired GS transport in the setting of isoflurane-induced enlargement of the venous sinuses (8). It is likely therefore, that high-altitude induced global vasodilation will negatively impact CSF influx and therefore GS transport.
- **Heart rate and respiration**: Clinical research studies in healthy subjects have shown that during ascent to high altitude heart rate and ventilation increase (31, 90, 101). The increased heart rate is caused by the associated hypoxemia (e.g., PaO_2 lower than 50 mmHg has been documented at 12-15,000 ft (31)) and is chemoreflex instigated via chemosensitive cells located in the carotid bodies and the aortic body (42). Similarly, the increased minute ventilation (primarily increased tidal volume) at high altitude is also primarily mediated via low arterial O_2 and stimulation of the chemoreceptors (42). A

moderate increase in heart rate would in principle increase CSF influx and facilitate enhanced CSF-ISF exchange (48). However, the more influential physiological driver of CSF dynamics at high altitude is likely to be an increase in respiratory tidal volume. Thus, human studies have shown that voluntary deep inspiratory breathing is a major driver CSF fluid flow through the cerebral ventricles and basal cisterns (27). The mechanism underlying deep inspiratory breathing on accelerating CSF flow dynamics is related to a more negative thoracic pressure during inspiration which will directly impact hydrostatic pressure gradients for flow along the perivenous conduits into meningeal lymphatics (27). Furthermore, a recent study showed that during normal human sleep, slow oscillating neural activity precedes coupled waves of blood and CSF flow in the brain (33). Thus, based on these data one might hypothesize that at high altitude, the beneficial effects of increased respiratory tidal volume on CSF fluid flow would serve to counteract the negative effects of nocturnal hypoxemia and restless sleep (31) on overall waste drainage. More studies are needed to explore the potential beneficial effect of maximizing deep inspiratory breathing at high altitude for prevention of AMS.

- **Brain swelling**: Increased blood volume and brain volume increases is documented in high altitude illness (38, 56). In HACE, vasogenic edema (evaluated by MRI and T2 relaxation) has been documented in deep white matter (corpus callosum) (41). However, whether or not cytotoxic edema occurs in AMS or HACE is contentious. In AMS one study documented very small increases in T2 values in the splenium of the corpus callosum with exposure to hypoxia (56). The same study also reported that the apparent diffusion coefficient (ADC) increased during the hypoxic episode in most brain regions but in AMS subjects minor decreases in the ADC was documented, which suggest the

presence of cytotoxic edema (56). Regardless, 'brain swelling' in high-altitude illness is associated with displacement of CSF (94, 108). These data strongly suggest that CSF transport from the subarachnoid space into peri-arterial conduits in the brain parenchyma is compromised in high-altitude illness and CSF-ISF exchange and waste clearance will consequently decline. Further, the formation of edema will further compromise cerebral perfusion eventually causing ischemia thereby instigating a vicious cycle towards aggravating the insult. It is tempting to speculate that the diversion of CSF away from brain parenchyma in the case of 'brain swelling' in high altitude sickness might be advantageous. CSF can certainly exit from the cranium without having to pass through the brain parenchyma (23, 53) and these alternate pathways would facilitate maintaining lower ICP. Intriguingly, cisternotomy and diversion of CSF (referred to clinically as "CSF-shift edema") in severe cases of TBI has been shown to decrease brain swelling, mortality and morbidity in afflicted subjects (15, 16).

- **Sleep disturbances:** Interrupted sleep and sleep disturbances have been documented in humans at high altitude (52, 84, 95). A recent metanalysis highlighting polysomnographic sleep studies revealed a reduction in non-rapid eye movement (NREM) sleep and reduction in slow wave sleep at high altitude (10). Because GS transport is most efficient during slow wave sleep (109) it could be inferred that brain waste drainage is impaired in subjects with restless sleep at high altitude, and thus potentially contribute to the pathogenesis of acute mountain sickness (AMS). In support, a recent positron emission tomography (PET) study using a radioactive Aβ ligand showed increased uptake of Aβ in the brain of healthy human subjects after one night of sleep deprivation (98). Furthermore, a clinical research study conducted at high altitude,

391 demonstrated that hypoxemia, unstable nocturnal ventilation (central apnea), and restless
392 sleep were early symptoms in subjects who later developed AMS (31). There is currently
393 a gap in knowledge regarding the effect of central or obstructive sleep apnea (OSA) on
394 GS transport. However, increased perivascular space visibility on brain MRI images – a
395 marker of cerebral small vessel disease (11, 106) - is associated with OSA (17, 102)
396 suggesting perivascular space dysfunction and indirectly inferring glymphatic transport
397 impairment (106). Clearly, more studies on the impact of obstructive and central sleep
398 apneas on CSF transport, GS transport and waste drainage are needed to the further
399 understanding of the pathogenesis of AMS.
400
401 In conclusion, the current conception of how the glymphatic system operates in the central
402 nervous system (CNS) under normal conditions and in states of neurodegeneration was reviewed
403 here. We also revealed that there is limited information on how states of hypoxia affects GS
404 solute transport and waste drainage in the live brain. Further, the reader must be aware that most
405 of the discussion and data pertaining to hypoxia and pathophysiology of AMS from the point of
406 view of GS transport are based on experiments conducted in rodents. Currently, a major barrier
407 to understanding GS transport is the lack of non-invasive imaging technologies for accurate
408 tracking solute transport and waste drainage in the human CNS. Future research efforts should
409 focus on developing sensitive and specific biomarkers for tracking aberrant CSF fluid flow
410 dynamics and endogenous waste drainage in real time.
411
412

References:

1. **Abbott NJ, Pizzo ME, Preston JE, Janigro D, and Thorne RG**. The role of brain barriers in fluid movement in the CNS: is there a 'glymphatic' system? *Acta Neuropathol* 135: 387-407, 2018.

2. **Absinta M, Ha SK, Nair G, Sati P, Luciano NJ, Palisoc M, Louveau A, Zaghloul KA, Pittaluga S, Kipnis J, and Reich DS**. Human and nonhuman primate meninges harbor lymphatic vessels that can be visualized noninvasively by MRI. *Elife* 6: 2017.

3. **Antila S, Karaman S, Nurmi H, Airavaara M, Voutilainen MH, Mathivet T, Chilov D, Li Z, Koppinen T, Park JH, Fang S, Aspelund A, Saarma M, Eichmann A, Thomas JL, and Alitalo K**. Development and plasticity of meningeal lymphatic vessels. *The Journal of experimental medicine* 214: 3645-3667, 2017.

4. **Aspelund A, Antila S, Proulx ST, Karlsen TV, Karaman S, Detmar M, Wiig H, and Alitalo K**. A dural lymphatic vascular system that drains brain interstitial fluid and macromolecules. *The Journal of experimental medicine* 212: 991-999, 2015.

5. **Bedussi B, Naessens DM, de Vos J, Olde Engberink R, Wilhelmus MM, Richard E, Ten Hove M, vanBavel E, and Bakker EN**. Enhanced interstitial fluid drainage in the hippocampus of spontaneously hypertensive rats. *Sci Rep* 7: 744, 2017.

6. **Bedussi B, Naessens DMP, de Vos J, Olde Engberink R, Wilhelmus MMM, Richard E, Ten Hove M, vanBavel E, and Bakker E**. Enhanced interstitial fluid drainage in the hippocampus of spontaneously hypertensive rats. *Sci Rep* 7: 744, 2017.

7. **Benamou JD, and Brenier Y**. A computational fluid mechanics solution to the Monge-Kantorovic mass transfer problem. *Numirische Mathematik* 84: 375-393, 2000.

8. **Benveniste H, Lee H, Ding F, Sun Q, Al-Bizri E, Makaryus R, Probst S, Nedergaard M, Stein EA, and Lu H**. Anesthesia with Dexmedetomidine and Low-dose Isoflurane Increases Solute Transport via the Glymphatic Pathway in Rat Brain When Compared with High-dose Isoflurane. *Anesthesiology* 127: 976-988, 2017.

9. **Benveniste H, Lee H, and Volkow ND**. The Glymphatic Pathway: Waste Removal from the CNS via Cerebrospinal Fluid Transport. *Neuroscientist* 23: 454-465, 2017.

10. **Bloch KE, Buenzli JC, Latshang TD, and Ulrich S**. Sleep at high altitude: guesses and facts. *J Appl Physiol (1985)* 119: 1466-1480, 2015.

11. **Brown R, Benveniste H, Black SE, Charpak S, Dichgans M, Joutel A, Nedergaard M, Smith KJ, Zlokovic BV, and Wardlaw JM**. Understanding the role of the perivascular space in cerebral small vessel disease. *Cardiovasc Res* 114: 1462-1473, 2018.

12. **Bucchieri F, Farina F, Zummo G, and Cappello F**. Lymphatic vessels of the dura mater: a new discovery? *J Anat* 227: 702-703, 2015.

13. **Callado LF, and Stamford JA**. Alpha2A- but not alpha2B/C-adrenoceptors modulate noradrenaline release in rat locus coeruleus: voltammetric data. *Eur J Pharmacol* 366: 35-39, 1999.

14. **Charles A**. The pathophysiology of migraine: implications for clinical management. *Lancet Neurol* 17: 174-182, 2018.

15. **Cherian I, Beltran M, Landi A, Alafaci C, Torregrossa F, and Grasso G**. Introducing the concept of "CSF-shift edema" in traumatic brain injury. *J Neurosci Res* 96: 744-752, 2018.

16. **Cherian I, Bernardo A, and Grasso G**. Cisternostomy for Traumatic Brain Injury: Pathophysiologic Mechanisms and Surgical Technical Notes. *World Neurosurg* 89: 51-57, 2016.

17. **Chokesuwattanaskul A, Lertjitbanjong P, Thongprayoon C, Bathini T, Sharma K, Mao MA, Cheungpasitporn W, and Chokesuwattanaskul R**. Impact of obstructive sleep apnea on silent cerebral small vessel disease: a systematic review and meta-analysis. *Sleep Med* 68: 80-88, 2020.

18. **Colantuoni A, Bertuglia S, and Intaglietta M**. Effects of anesthesia on the spontaneous activity of the microvasculature. *Int J Microcirc Clin Exp* 3: 13-28, 1984.

19. **Crone C**. Transport of solutes and water across the blood-brain barrier [proceedings]. *J Physiol* 266: 34P-35P, 1977.

20. **Cserr HF**. Relationship between cerebrospinal fluid and interstitial fluid of brain. *Fed Proc* 33: 2075-2078, 1974.

21. **Da Mesquita S, Louveau A, Vaccari A, Smirnov I, Cornelison RC, Kingsmore KM, Contarino C, Onengut-Gumuscu S, Farber E, Raper D, Viar KE, Powell RD, Baker W, Dabhi N, Bai R, Cao R, Hu S, Rich SS, Munson JM, Lopes MB, Overall CC, Acton ST, and Kipnis J**. Functional aspects of meningeal lymphatics in ageing and Alzheimer's disease. *Nature* 560: 185-191, 2018.

22. **De Guio F, Jouvent E, Biessels GJ, Black SE, Brayne C, Chen C, Cordonnier C, De Leeuw FE, Dichgans M, Doubal F, Duering M, Dufouil C, Duzel E, Fazekas F, Hachinski**

V, Ikram MA, Linn J, Matthews PM, Mazoyer B, Mok V, Norrving B, O'Brien JT, Pantoni L, Ropele S, Sachdev P, Schmidt R, Seshadri S, Smith EE, Sposato LA, Stephan B, Swartz RH, Tzourio C, van Buchem M, van der Lugt A, van Oostenbrugge R, Vernooij MW, Viswanathan A, Werring D, Wollenweber F, Wardlaw JM, and Chabriat H. Reproducibility and variability of quantitative magnetic resonance imaging markers in cerebral small vessel disease. *J Cereb Blood Flow Metab* 36: 1319-1337, 2016.

23. **de Leon MJ, Li Y, Okamura N, Tsui WH, Saint-Louis LA, Glodzik L, Osorio RS, Fortea J, Butler T, Pirraglia E, Fossati S, Kim HJ, Carare RO, Nedergaard M, Benveniste H, and Rusinek H**. Cerebrospinal Fluid Clearance in Alzheimer Disease Measured with Dynamic PET. *Journal of nuclear medicine : official publication, Society of Nuclear Medicine* 58: 1471-1476, 2017.

24. **Desai RA, Davies AL, Tachrount M, Kasti M, Laulund F, Golay X, and Smith KJ**. Cause and prevention of demyelination in a model multiple sclerosis lesion. *Ann Neurol* 79: 591-604, 2016.

25. **Di Marco LY, Farkas E, Martin C, Venneri A, and Frangi AF**. Is Vasomotion in Cerebral Arteries Impaired in Alzheimer's Disease? *J Alzheimers Dis* 46: 35-53, 2015.

26. **Doubal FN, MacLullich AM, Ferguson KJ, Dennis MS, and Wardlaw JM**. Enlarged perivascular spaces on MRI are a feature of cerebral small vessel disease. *Stroke* 41: 450-454, 2010.

27. **Dreha-Kulaczewski S, Joseph AA, Merboldt KD, Ludwig HC, Gartner J, and Frahm J**. Inspiration is the major regulator of human CSF flow. *The Journal of neuroscience : the official journal of the Society for Neuroscience* 35: 2485-2491, 2015.

28. **Eide PK, and Ringstad G**. Delayed clearance of cerebrospinal fluid tracer from entorhinal cortex in idiopathic normal pressure hydrocephalus: A glymphatic magnetic resonance imaging study. *J Cereb Blood Flow Metab* 271678X18760974, 2018.

29. **Eide PK, and Ringstad G**. MRI with intrathecal MRI gadolinium contrast medium administration: a possible method to assess glymphatic function in human brain. *Acta Radiol Open* 4: 2058460115609635, 2015.

30. **Elkin R, Nadeem S, Haber E, Steklova K, Lee H, Benveniste H, and Tannenbaum A**. GlymphVIS: Visualizing glymphatic transport pathways using regularized optimal transport. *Med Image Comput Comput Assist Interv* 11070: 844-852, 2018.

31. **Erba P, Anastasi S, Senn O, Maggiorirni M, and Bloch KE**. Acute mountain sickness is related to nocturnal hypoxemia but not to hypoventilation. *Eur Respir J* 24: 303-308, 2004.

32. **Fisher CM**. Lacunar strokes and infarcts: a review. *Neurology* 32: 871-876, 1982.

33. **Fultz NE, Bonmassar G, Setsompop K, Stickgold RA, Rosen BR, Polimeni JR, and Lewis LD**. Coupled electrophysiological, hemodynamic, and cerebrospinal fluid oscillations in human sleep. *Science* 366: 628-631, 2019.

34. **Gaberel T, Gakuba C, Goulay R, Martinez De Lizarrondo S, Hanouz JL, Emery E, Touze E, Vivien D, and Gauberti M**. Impaired glymphatic perfusion after strokes revealed by contrast-enhanced MRI: a new target for fibrinolysis? *Stroke* 45: 3092-3096, 2014.

35. **Garyfallidis E, Brett M, Correia MM, Williams GB, and Nimmo-Smith I**. QuickBundles, a Method for Tractography Simplification. *Front Neurosci* 6: 175, 2012.

516 36. **Goodman JR, Adham ZO, Woltjer RL, Lund AW, and Iliff JJ**. Characterization of
517 dural sinus-associated lymphatic vasculature in human Alzheimer's dementia subjects. *Brain*
518 *Behav Immun* 73: 34-40, 2018.

519 37. **Goulay R, Flament J, Gauberti M, Naveau M, Pasquet N, Gakuba C, Emery E,**
520 **Hantraye P, Vivien D, Aron-Badin R, and Gaberel T**. Subarachnoid Hemorrhage Severely
521 Impairs Brain Parenchymal Cerebrospinal Fluid Circulation in Nonhuman Primate. *Stroke* 48:
522 2301-2305, 2017.

523 38. **Hackett PH**. The cerebral etiology of high-altitude cerebral edema and acute mountain
524 sickness. *Wilderness Environ Med* 10: 97-109, 1999.

525 39. **Hackett PH, Rennie D, and Levine HD**. The incidence, importance, and prophylaxis of
526 acute mountain sickness. *Lancet* 2: 1149-1155, 1976.

527 40. **Hackett PH, and Roach RC**. High-altitude illness. *N Engl J Med* 345: 107-114, 2001.

528 41. **Hackett PH, Yarnell PR, Hill R, Reynard K, Heit J, and McCormick J**. High-altitude
529 cerebral edema evaluated with magnetic resonance imaging: clinical correlation and
530 pathophysiology. *JAMA* 280: 1920-1925, 1998.

531 42. **Hall JE, and Guyton AC**. *Guyton and Hall textbook of medical physiology*.
532 Philadelphia, PA: Saunders/Elsevier, 2011, p. xix, 1091p.

533 43. **Hudetz AG, Biswal BB, Shen H, Lauer KK, and Kampine JP**. Spontaneous
534 fluctuations in cerebral oxygen supply. An introduction. *Adv Exp Med Biol* 454: 551-559, 1998.

535 44. **Iliff JJ, Chen MJ, Plog BA, Zeppenfeld DM, Soltero M, Yang L, Singh I, Deane R,**
536 **and Nedergaard M**. Impairment of glymphatic pathway function promotes tau pathology after

traumatic brain injury. *The Journal of neuroscience : the official journal of the Society for Neuroscience* 34: 16180-16193, 2014.

45. **Iliff JJ, Lee H, Yu M, Feng T, Logan J, Nedergaard M, and Benveniste H**. Brain-wide pathway for waste clearance captured by contrast-enhanced MRI. *J Clin Invest* 123: 1299-1309, 2013.

46. **Iliff JJ, and Nedergaard M**. Is there a cerebral lymphatic system? *Stroke* 44: S93-95, 2013.

47. **Iliff JJ, Wang M, Liao Y, Plogg BA, Peng W, Gundersen GA, Benveniste H, Vates GE, Deane R, Goldman SA, Nagelhus EA, and Nedergaard M**. A paravascular pathway facilitates CSF flow through the brain parenchyma and the clearance of interstitial solutes, including amyloid beta. *Science translational medicine* 4: 147ra111, 2012.

48. **Iliff JJ, Wang M, Zeppenfeld DM, Venkataraman A, Plog BA, Liao Y, Deane R, and Nedergaard M**. Cerebral arterial pulsation drives paravascular CSF-interstitial fluid exchange in the murine brain. *The Journal of neuroscience : the official journal of the Society for Neuroscience* 33: 18190-18199, 2013.

49. **Intaglietta M**. Arteriolar vasomotion: implications for tissue ischemia. *Blood Vessels* 28 Suppl 1: 1-7, 1991.

50. **Jiang Q, Zhang L, Ding G, Davoodi-Bojd E, Li Q, Li L, Sadry N, Nedergaard M, Chopp M, and Zhang Z**. Impairment of the glymphatic system after diabetes. *J Cereb Blood Flow Metab* 37: 1326-1337, 2017.

51. **Jochems ACC, Blair GW, Stringer MS, Thrippleton MJ, Clancy U, Chappell FM, Brown R, Jaime Garcia D, Hamilton OKL, Morgan AG, Marshall I, Hetherington K, Wiseman S, MacGillivray T, Valdes-Hernandez MC, Doubal FN, and Wardlaw JM**. Relationship Between Venules and Perivascular Spaces in Sporadic Small Vessel Diseases. *Stroke* 51: 1503-1506, 2020.

52. **Johnson PL, Edwards N, Burgess KR, and Sullivan CE**. Sleep architecture changes during a trek from 1400 to 5000 m in the Nepal Himalaya. *J Sleep Res* 19: 148-156, 2010.

53. **Johnston M, Zakharov A, Papaiconomou C, Salmasi G, and Armstrong D**. Evidence of connections between cerebrospinal fluid and nasal lymphatic vessels in humans, non-human primates and other mammalian species. *Cerebrospinal Fluid Res* 1: 2, 2004.

54. **Jorm CM, and Stamford JA**. Actions of the hypnotic anaesthetic, dexmedetomidine, on noradrenaline release and cell firing in rat locus coeruleus slices. *Br J Anaesth* 71: 447-449, 1993.

55. **Kalaria R, Ferrer I, and Love S**. Vascular Disease, Hypoxia and Related Conditions. In: *Greenfield's Neuropathology*, edited by Love S, Perry A, Ironside J, and Budka H. Boca Raton, FL: CRC Press, 2015, p. 91-125.

56. **Kallenberg K, Bailey DM, Christ S, Mohr A, Roukens R, Menold E, Steiner T, Bartsch P, and Knauth M**. Magnetic resonance imaging evidence of cytotoxic cerebral edema in acute mountain sickness. *J Cereb Blood Flow Metab* 27: 1064-1071, 2007.

57. **Kari HP, Davidson PP, Kohl HH, and Kochhar MM**. Effects of ketamine on brain monoamine levels in rats. *Res Commun Chem Pathol Pharmacol* 20: 475-488, 1978.

58. **Kida S, and Weller RO**. Morphological basis for fluid transport through and around ependymal, arachnoidal and glial cells. In: *principles of pediatric neuroscurgery, Vol IW, intracranial cyste lesions*, edited by Raimondi A. Berlin: Springer-Verlag, 1993, p. 37-52.

59. **Klingelhöfer J**. Cerebral blood flow velocity in sleep. *Perspectives in Medicine* 1: 275-284, 2012.

60. **Kotajima F, Meadows GE, Morrell MJ, and Corfield DR**. Cerebral blood flow changes associated with fluctuations in alpha and theta rhythm during sleep onset in humans. *J Physiol* 568: 305-313, 2005.

61. **Koundal S, Elkin R, Nadeem S, Xue Y, Constantinou S, Sanggaard S, Liu X, Monte B, Xu F, Van Nostrand W, Nedergaard M, Lee H, Wardlaw J, Benveniste H, and Tannenbaum A**. Optimal Mass Transport with Lagrangian Workflow Reveals Advective and Diffusion Driven Solute Transport in the Glymphatic System. *Sci Rep* 10: 1990, 2020.

62. **Kress BT, Iliff JJ, Xia M, Wang M, Wei HS, Zeppenfeld D, Xie L, Kang H, Xu Q, Liew JA, Plog BA, Ding F, Deane R, and Nedergaard M**. Impairment of paravascular clearance pathways in the aging brain. *Ann Neurol* 76: 845-861, 2014.

63. **Kubota T, Hirota K, Yoshida H, Takahashi S, Anzawa N, Ohkawa H, Kushikata T, and Matsuki A**. Effects of sedatives on noradrenaline release from the medial prefrontal cortex in rats. *Psychopharmacology (Berl)* 146: 335-338, 1999.

64. **Lamblin V, Favory R, Boulo M, and Mathieu D**. Microcirculatory alterations induced by sedation in intensive care patients. Effects of midazolam alone and in association with sufentanil. *Crit Care* 10: R176, 2006.

65. **Lawley JS, Levine BD, Williams MA, Malm J, Eklund A, Polaner DM, Subudhi AW, Hackett PH, and Roach RC**. Cerebral spinal fluid dynamics: effect of hypoxia and implications for high-altitude illness. *J Appl Physiol (1985)* 120: 251-262, 2016.

66. **Lee H, Mortensen K, Sanggaard S, Koch P, Brunner H, Quistorff B, Nedergaard M, and Benveniste H**. Quantitative Gd-DOTA uptake from cerebrospinal fluid into rat brain using 3D VFA-SPGR at 9.4T. *Magn Reson Med* 79: 1568-1578, 2018.

67. **Lee H, Xie L, Yu M, Kang H, Feng T, Deane R, Logan J, Nedergaard M, and Benveniste H**. The Effect of Body Posture on Brain Glymphatic Transport. *The Journal of neuroscience : the official journal of the Society for Neuroscience* 35: 11034-11044, 2015.

68. **Liu W, Liu J, Lou X, Zheng D, Wu B, Wang DJ, and Ma L**. A longitudinal study of cerebral blood flow under hypoxia at high altitude using 3D pseudo-continuous arterial spin labeling. *Sci Rep* 7: 43246, 2017.

69. **Louveau A, Smirnov I, Keyes TJ, Eccles JD, Rouhani SJ, Peske JD, Derecki NC, Castle D, Mandell JW, Lee KS, Harris TH, and Kipnis J**. Structural and functional features of central nervous system lymphatic vessels. *Nature* 523: 337-341, 2015.

70. **Lowe J, and Kalaria R**. Dementia. In: *Greenfield's Neuropathology*, edited by Love S, Perry A, Ironside J, and Budka HCRC Press, 2015, p. 858-953.

71. **Ma Q, Ineichen BV, Detmar M, and Proulx ST**. Outflow of cerebrospinal fluid is predominantly through lymphatic vessels and is reduced in aged mice. *Nat Commun* 8: 1434, 2017.

72. **Madsen PL, and Vorstrup S**. Cerebral blood flow and metabolism during sleep. *Cerebrovasc Brain Metab Rev* 3: 281-296, 1991.

73. **Martinez Sosa S, and Smith KJ**. Understanding a role for hypoxia in lesion formation and location in the deep and periventricular white matter in small vessel disease and multiple sclerosis. *Clin Sci (Lond)* 131: 2503-2524, 2017.

74. **Mathiisen TM, Lehre KP, Danbolt NC, and Ottersen OP**. The perivascular astroglial sheath provides a complete covering of the brain microvessels: an electron microscopic 3D reconstruction. *Glia* 58: 1094-1103, 2010.

75. **Mefford IN, and Garrick NA**. Effects of xylazine on cerebrospinal fluid catecholamines in the rhesus monkey. *Brain Res* 492: 377-380, 1989.

76. **Mestre H, Hablitz LM, Xavier AL, Feng W, Zou W, Pu T, Monai H, Murlidharan G, Castellanos Rivera RM, Simon MJ, Pike MM, Pla V, Du T, Kress BT, Wang X, Plog BA, Thrane AS, Lundgaard I, Abe Y, Yasui M, Thomas JH, Xiao M, Hirase H, Asokan A, Iliff JJ, and Nedergaard M**. Aquaporin-4-dependent glymphatic solute transport in the rodent brain. *Elife* 7: 2018.

77. **Mestre H, Kostrikov S, Mehta RI, and Nedergaard M**. Perivascular spaces, glymphatic dysfunction, and small vessel disease. *Clin Sci (Lond)* 131: 2257-2274, 2017.

78. **Mestre H, Tithof J, Du T, Song W, Peng W, Sweeney AM, Olveda G, Thomas JH, Nedergaard M, and Kelley DH**. Flow of cerebrospinal fluid is driven by arterial pulsations and is reduced in hypertension. *Nat Commun* 9: 4878, 2018.

79. **Mortensen KN, Sanggaard S, Mestre H, Lee H, Kostrikov S, Xavier ALR, Gjedde A, Benveniste H, and Nedergaard M**. Impaired Glymphatic Transport in Spontaneously Hypertensive Rats. *The Journal of neuroscience : the official journal of the Society for Neuroscience* 39: 6365-6377, 2019.

80. **Ohene Y, Harrison IF, Nahavandi P, Ismail O, Bird EV, Ottersen OP, Nagelhus EA, Thomas DL, Lythgoe MF, and Wells JA**. Non-invasive MRI of brain clearance pathways using multiple echo time arterial spin labelling: an aquaporin-4 study. *Neuroimage* 188: 515-523, 2019.

81. **Peng W, Achariyar TM, Li B, Liao Y, Mestre H, Hitomi E, Regan S, Kasper T, Peng S, Ding F, Benveniste H, Nedergaard M, and Deane R**. Suppression of glymphatic fluid transport in a mouse model of Alzheimer's disease. *Neurobiology of disease* 93: 215-225, 2016.

82. **Pizzo ME, Wolak DJ, Kumar NN, Brunette E, Brunnquell CL, Hannocks MJ, Abbott NJ, Meyerand ME, Sorokin L, Stanimirovic DB, and Thorne RG**. Intrathecal antibody distribution in the rat brain: surface diffusion, perivascular transport and osmotic enhancement of delivery. *J Physiol* 596: 445-475, 2018.

83. **Plog BA, Dashnaw ML, Hitomi E, Peng W, Liao Y, Lou N, Deane R, and Nedergaard M**. Biomarkers of traumatic injury are transported from brain to blood via the glymphatic system. *The Journal of neuroscience : the official journal of the Society for Neuroscience* 35: 518-526, 2015.

84. **Plywaczewski R, Wu TY, Wang XQ, Cheng HW, Sliwinski PS, and Zielinski J**. Sleep structure and periodic breathing in Tibetans and Han at simulated altitude of 5000 m. *Respir Physiol Neurobiol* 136: 187-197, 2003.

85. **Rachev ST, and Rüschendorf L**. *Mass Transportation Problems*. Springer, 1998.

86. **Ratner V, Gao Y, Lee H, Elkin R, Nedergaard M, Benveniste H, and Tannenbaum A**. Cerebrospinal and interstitial fluid transport via the glymphatic pathway modeled by optimal mass transport. *Neuroimage* 152: 530-537, 2017.

87. **Ratner V, Zhu L, Kolesov I, Nedergaard M, Benveniste H, and Tannenbaum A**. Optimal-mass-transfer-based estimation of glymphatic transport in living brain. *Proceedings of SPIE--the International Society for Optical Engineering* 9413: 2015.

88. **Ren Z, Iliff JJ, Yang L, Yang J, Chen X, Chen MJ, Giese RN, Wang B, Shi X, and Nedergaard M**. 'Hit & Run' model of closed-skull traumatic brain injury (TBI) reveals complex patterns of post-traumatic AQP4 dysregulation. *J Cereb Blood Flow Metab* 33: 834-845, 2013.

89. **Rennels ML, Gregory TF, Blaumanis OR, Fujimoto K, and Grady PA**. Evidence for a 'paravascular' fluid circulation in the mammalian central nervous system, provided by the rapid distribution of tracer protein throughout the brain from the subarachnoid space. *Brain Res* 326: 47-63, 1985.

90. **Richalet JP, and Lhuissier FJ**. Aging, Tolerance to High Altitude, and Cardiorespiratory Response to Hypoxia. *High Alt Med Biol* 16: 117-124, 2015.

91. **Ringstad G, Valnes LM, Dale AM, Pripp AH, Vatnehol SS, Emblem KE, Mardal KA, and Eide PK**. Brain-wide glymphatic enhancement and clearance in humans assessed with MRI. *JCI Insight* 3: 2018.

92. **Ringstad G, Vatnehol SAS, and Eide PK**. Glymphatic MRI in idiopathic normal pressure hydrocephalus. *Brain : a journal of neurology* 140: 2691-2705, 2017.

93. **Roach RC, Houston CS, Honigman B, Nicholas RA, Yaron M, Grissom CK, Alexander JK, and Hultgren HN**. How well do older persons tolerate moderate altitude? *West J Med* 162: 32-36, 1995.

94. **Ross RT**. The random nature of cerebral mountain sickness. *Lancet* 1: 990-991, 1985.

95. **Salvaggio A, Insalaco G, Marrone O, Romano S, Braghiroli A, Lanfranchi P, Patruno V, Donner CF, and Bonsignore G**. Effects of high-altitude periodic breathing on sleep and arterial oxyhaemoglobin saturation. *Eur Respir J* 12: 408-413, 1998.

96. **Sawaya R, and Ingvar DH**. Cerebral blood flow and metabolism in sleep. *Acta Neurol Scand* 80: 481-491, 1989.

97. **Shi Y, and Wardlaw JM**. Update on cerebral small vessel disease: a dynamic whole-brain disease. *Stroke Vasc Neurol* 1: 83-92, 2016.

98. **Shokri-Kojori E, Wang GJ, Wiers CE, Demiral SB, Guo M, Kim SW, Lindgren E, Ramirez V, Zehra A, Freeman C, Miller G, Manza P, Srivastava T, De Santi S, Tomasi D, Benveniste H, and Volkow ND**. beta-Amyloid accumulation in the human brain after one night of sleep deprivation. *Proc Natl Acad Sci U S A* 115: 4483-4488, 2018.

99. **Simon MJ, and Iliff JJ**. Regulation of cerebrospinal fluid (CSF) flow in neurodegenerative, neurovascular and neuroinflammatory disease. *Biochim Biophys Acta* 1862: 442-451, 2016.

100. **Smith AJ, Yao X, Dix JA, Jin BJ, and Verkman AS**. Test of the 'glymphatic' hypothesis demonstrates diffusive and aquaporin-4-independent solute transport in rodent brain parenchyma. *Elife* 6: 2017.

101. **Snyder EM, Stepanek J, Bishop SL, and Johnson BD**. Ventilatory responses to hypoxia and high altitude during sleep in Aconcagua climbers. *Wilderness Environ Med* 18: 138-145, 2007.

102. **Song TJ, Park JH, Choi KH, Chang Y, Moon J, Kim JH, Choi Y, Kim YJ, and Lee HW**. Moderate-to-severe obstructive sleep apnea is associated with cerebral small vessel disease. *Sleep Med* 30: 36-42, 2017.

103. **Sun BL, Wang LH, Yang T, Sun JY, Mao LL, Yang MF, Yuan H, Colvin RA, and Yang XY**. Lymphatic drainage system of the brain: A novel target for intervention of neurological diseases. *Prog Neurobiol* 163-164: 118-143, 2018.

104. **van Veluw SJ, Hou SS, Calvo-Rodriguez M, Arbel-Ornath M, Snyder AC, Frosch MP, Greenberg SM, and Bacskai BJ**. Vasomotion as a Driving Force for Paravascular Clearance in the Awake Mouse Brain. *Neuron* 105: 549-561 e545, 2020.

105. **Villien M, Bouzat P, Rupp T, Robach P, Lamalle L, Tropres I, Esteve F, Krainik A, Levy P, Warnking JM, and Verges S**. Changes in cerebral blood flow and vasoreactivity to CO2 measured by arterial spin labeling after 6days at 4350m. *Neuroimage* 72: 272-279, 2013.

106. **Wardlaw JM, Benveniste H, Nedergaard M, Zlokovic BV, Mestre H, Lee H, Doubal FN, Brown R, Ramirez J, MacIntosh BJ, Tannenbaum A, Ballerini L, Rungta RL, Boido D, Sweeney M, Montagne A, Charpak S, Joutel A, Smith KJ, Black SE, and colleagues from the Fondation Leducq Transatlantic Network of Excellence on the Role of the Perivascular Space in Cerebral Small Vessel D**. Perivascular spaces in the brain: anatomy, physiology and pathology. *Nat Rev Neurol* 16: 137-153, 2020.

107. **Wardlaw JM, Smith C, and Dichgans M**. Mechanisms of sporadic cerebral small vessel disease: insights from neuroimaging. *Lancet Neurol* 12: 483-497, 2013.

108. **Wilson MH, Davagnanam I, Holland G, Dattani RS, Tamm A, Hirani SP, Kolfschoten N, Strycharczuk L, Green C, Thornton JS, Wright A, Edsell M, Kitchen ND, Sharp DJ, Ham TE, Murray A, Holloway CJ, Clarke K, Grocott MP, Montgomery H, Imray C, Birmingham Medical Research Expeditionary S, and Caudwell Xtreme Everest Research G**. Cerebral venous system and anatomical predisposition to high-altitude headache. *Ann Neurol* 73: 381-389, 2013.

109. **Xie L, Kang H, Xu Q, Chen MJ, Liao Y, Thiyagarajan M, O'Donnell J, Christensen DJ, Nicholson C, Iliff JJ, Takano T, Deane R, and Nedergaard M**. Sleep drives metabolite clearance from the adult brain. *Science* 342: 373-377, 2013.

110. **Zhang Z, and Khatami R**. Predominant endothelial vasomotor activity during human sleep: a near-infrared spectroscopy study. *Eur J Neurosci* 40: 3396-3404, 2014.

744

745

746

747

748 **Legends:**

749 Fig. 1: T2-weigthed MRIs acquired on a 1.5T MRI instrument (GE Signa HDx 1.5using a T2 fast-
750 spin-echo pulse sequence (4-mm thick slices) from the brain of a healthy 35-year-old female.
751 Perivascular spaces are clearly visible (yellow arrows) in a typical pattern. Data courtesy:
752 Joanna Wardlaw.

753 Fig. 2: Illustration of the glymphatic system of the brain. In principle, the GS comprise a peri-
754 arterial influx pathway and a peri-venous pathway for CSF transit which are coupled to the
755 interstitial fluid (ISF) space via the aquaporin 4 (APP4) water channels. The AQP4 water
756 channels are positioned on the glial endfeet that make up the outer perimeter of the perivascular
757 space; the inner perimeter is the vascular basement membrane. CSF flows into the peri-arterial
758 space, and mixes with ISF whereby waste solutes (black particles) are propelled towards the
759 peri-venous conduits for ultimate drainage out of the brain.

760 Fig. 3: Glymphatic transport visualized by optimal mass transport (OMT) analysis based on
761 dynamic contrast enhanced MRIs obtained from a live rat after MR contrast administration into
762 the CSF. The OMT based analysis derives 'CSF transport pathlines' which are shown as a color-
763 coded map overlaid on the corresponding volume rendered anatomical MRI. We are showing the
764 effect of increasing the diffusion term in the optimal transport algorithm. Specifically, with a

765 minimal or absent diffusion term in the OMT analysis, the pattern of CSF parenchymal
766 streamlines do not align well with physiological evidence of MR contrast uptake in live rodent
767 brain (**Fig. 3A, arrows on non-existing CSF pathlines**). However, with more diffusion
768 'weighting' (**Fig. 3B**) the aberrant parenchymal CSF pathways have disappeared and the uptake
769 pattern better match what is observed on the MRI data, strongly suggesting that parenchymal GS
770 transport is governed by both advection and diffusion.

771 Fig. 4: **A** shows the conventional visualization of glymphatic transport in whole rat brain based
772 on dynamic contrast enhanced (DCE) MRIs expressed as '% signal increase from baseline' 1.5
773 hrs. after administration of MR contrast into the CSF via cisterna magna. The color-coded map
774 shows the spatial distribution of CSF tagged with MR contrast demonstrating that CSF and the
775 contrast solute have penetrated into the cerebellum, midbrain, olfactory bulb and along the PVS
776 of the middle cerebral artery as highlighted in **C**. **B** shows the same data set processed by the
777 GlymphVis algorithm with advection and diffusion terms deriving CSF streamlines. These
778 streamlines show brain parenchymal CSF flow patterns at a fixed point in time. Please note that
779 the CSF streamlines including transport along the MCA **(D)** are well matched to contrast uptake
780 in the original data (compare with **A, C**). Scale bars = 2 mm.

781

782

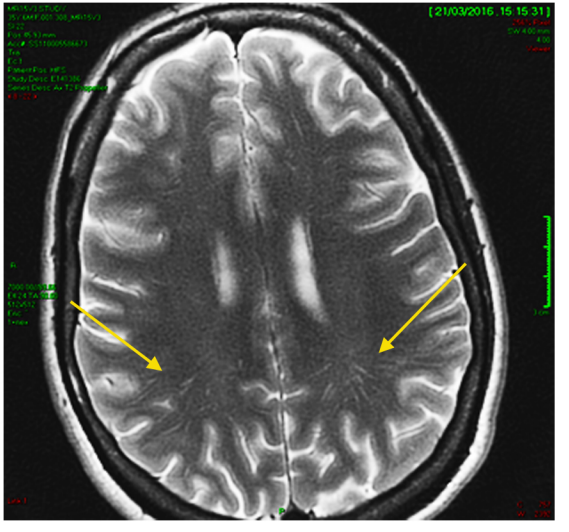
[21/03/2016 15:15:31]

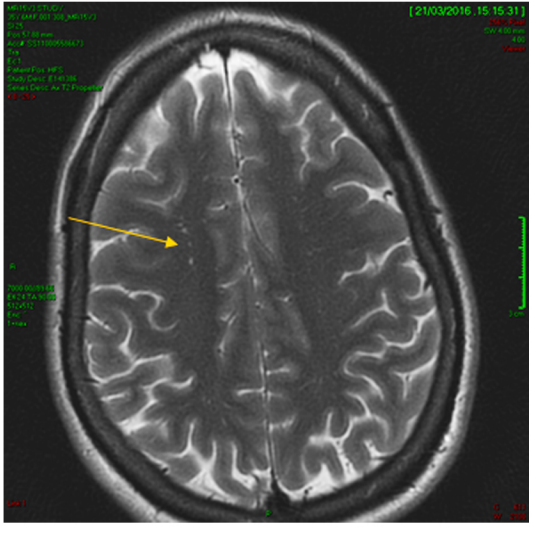
[21/03/2016 15:15:31]

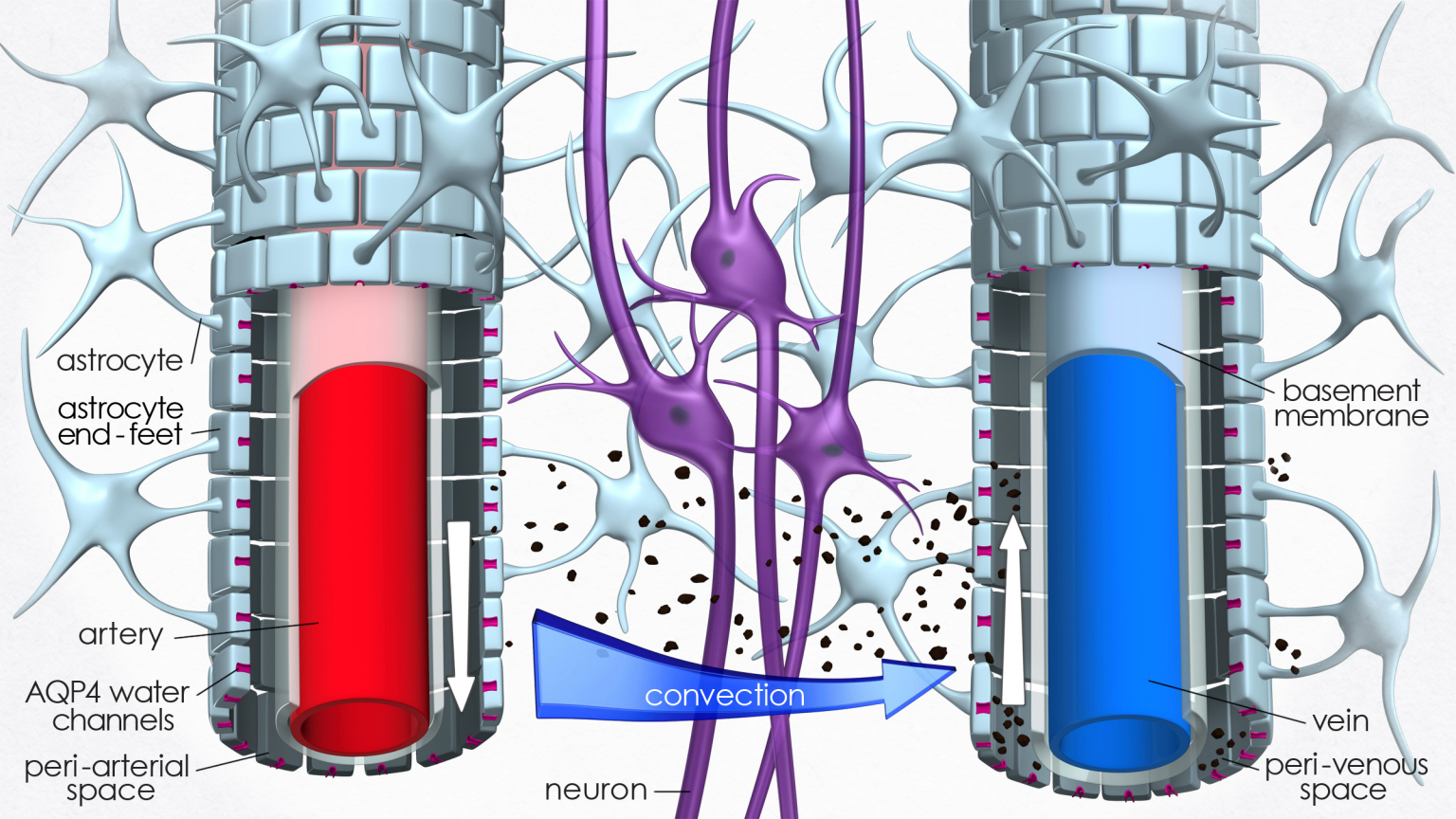
astrocyte
astrocyte end-feet
artery
AQP4 water channels
peri-arterial space
neuron
convection
basement membrane
vein
peri-venous space

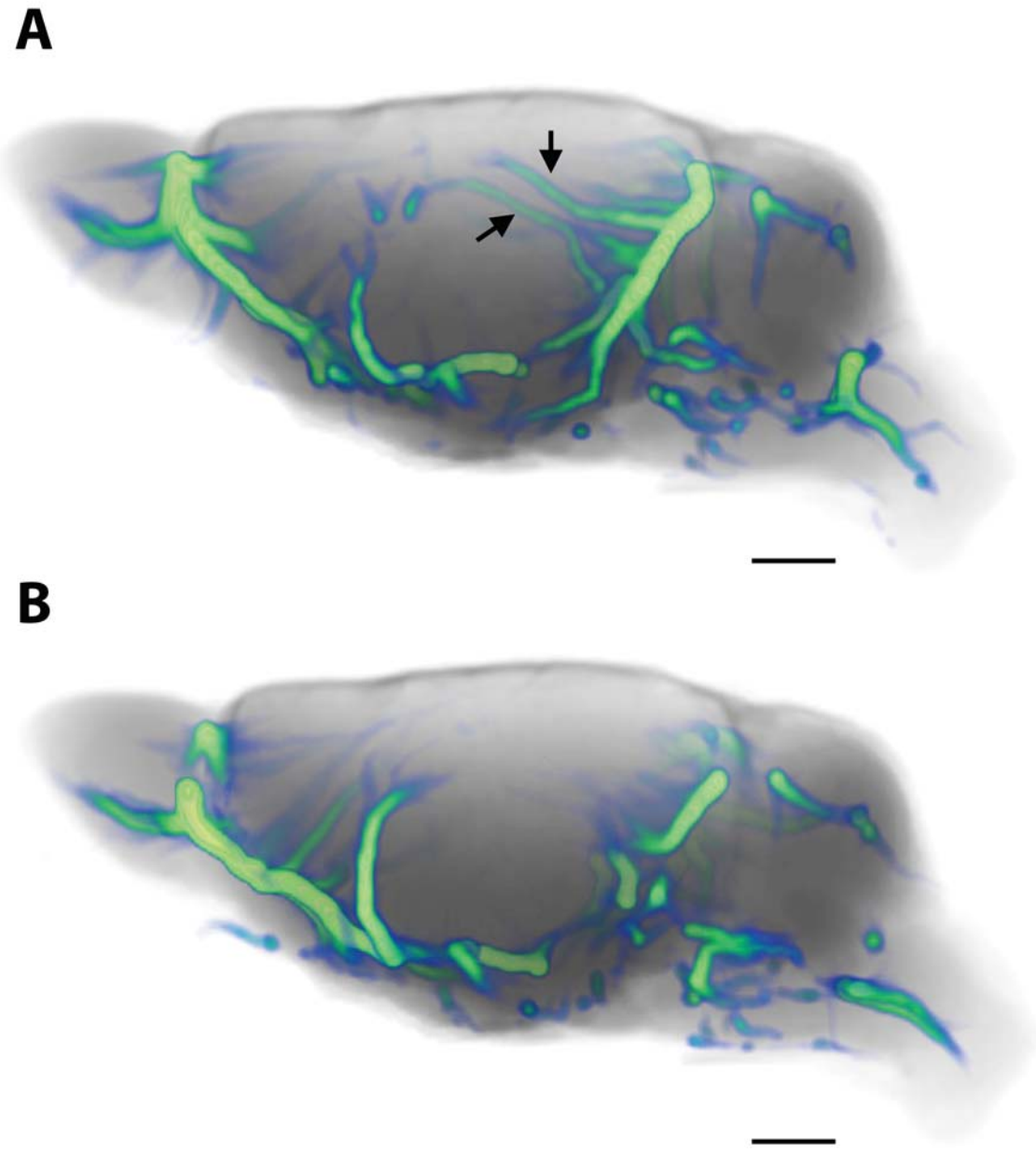
A
B

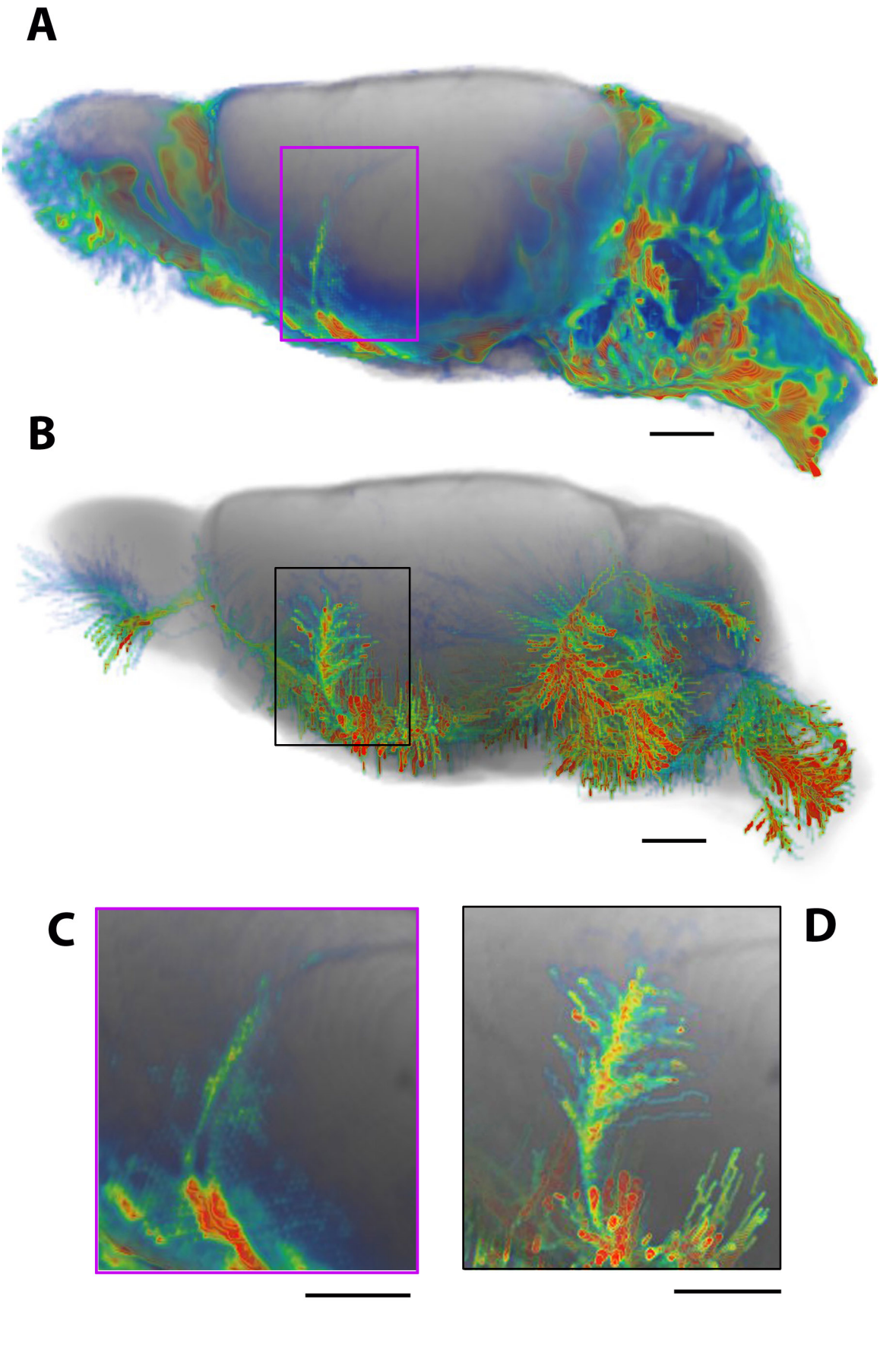
A
B
C
D